Applied Geography 52 (2014) 204–211

Contents lists available at ScienceDirect

Applied Geography

journal homepage: www.elsevier.com/locate/apgeog

Fractally deforested landscape: Pattern and process in a tri-national Amazon frontier

Jing Sun [a, *], Zhuojie Huang [b], Qiang Zhen [c], Jane Southworth [d], Stephen Perz [e]

[a] Center for Systems Integration and Sustainability, Michigan State University, East Lansing, MI 48823, USA
[b] GeoVISTA Center, Penn State University, 302 Walker, University Park, PA 16802, USA
[c] Department of Mathematics & Statistics, University of North Florida, Jacksonville, FL 32224, USA
[d] Department of Geography, University of Florida, Gainesville, FL 32611, USA
[e] Department of Sociology and Criminology & Law, University of Florida, Gainesville, FL 32611, USA

Keywords:
Amazon
Deforestation
Fractal analysis
Fixed-grid scans
Bottom-up plan
Configuration scheme

A B S T R A C T

Forest clearings in the Amazon are expanding along roads and are enhanced by the associated expansion of human settlements. The purpose of this research is to analyze the spatial patterns associated with this development process using fractal geometry and to partition this development process into different levels by a model-based classification scheme that can be applied to regions globally. A critical region of tropical forest cover in the tri-national frontier in the center of the southwestern Amazon was used as the study area. We utilized box-counting fractal dimensions to describe the spatial patterns of deforestation at a pixel level from 1986 to 2010 in the study region. The evolving pattern of development, as indicated by density-sliced fractal dimension, provides a unique and informative view of a deforesting landscape. The cleared areas have become increasingly compact from 1986 to 2010, where the low fractal dimensions typically represent little to no forest clearings and higher fractal dimensions are associated with more highly developed areas. Such differences are summarized by a classification scheme derived from a mathematical model that partitions the continuous range of fractal dimensions into five possible classes ranging from no or minimal development to highly developed. Such graphical representations of these stages of deforestation in the study region with such spatially explicit pixel-level information enables us to provide multi-level, local, adaptive, and flexible information to forest conservation groups, land managers and related programs.

Introduction

Human society is undergoing a rapid transformation associated with development that will eventually produce a post-industrial era and associated landscapes. Such drastic transitions have already produced potentially threatening changes in almost every aspect of our social-ecological systems (Gunderson & Holling, 2002), and abrupt global environmental changes can no longer be excluded (Scheffer et al., 2009; Scheffer, Carpenter, Foley, Folke, & Walker, 2001). Among them, land use and land cover changes are occurring globally and at increasingly unprecedented rates, impacting almost all major biomes worldwide (Gutman et al., 2004; Lambin & Geist, 2006). This is especially true of the process of large-scale deforestation occurring throughout the Amazon, which has received considerable attention over the past several decades (Laurance et al., 2002; Lima et al., 2012; Messina, Walsh, Mena, & Delamater, 2006; Nepstad et al., 2001).

Deforestation has a strong influence on regional and global climates (Malhi et al., 2008). For example, the consumption of the cleared forests (e.g., fuel wood) produces greenhouse gases, such as carbon dioxide, methane, and nitrous oxide, which play an important role in exacerbating global warming (Fearnside, 2004). Deforestation may also signal an impending biodiversity loss or even a biotic collapse (Nobre, Malagutti, Urbano, de Almeida, & Giarolla, 2009) caused by the loss of landscape connectivity, both structural and functional because the persistence of spatially structured species populations, or meta-populations, is strongly related to landscape connectivity (Hanski & Ovaskainen, 2003). However, the process of deforestation serves to increase forest fragmentation, breaking continuous forests into discrete patches

* Corresponding author.
E-mail addresses: jingsun@msu.edu, sunjingchanges@gmail.com (J. Sun), zxh6@psu.edu (Z. Huang), q.zhen@unf.edu (Q. Zhen), jsouthwo@ufl.edu (J. Southworth), sperz@ufl.edu (S. Perz).

http://dx.doi.org/10.1016/j.apgeog.2014.05.011
0143-6228/

and, over time, increasing the level of patch isolation (Sun & Southworth, 2013a). Thus, a lack of connectivity would reduce the capacity for species movement. The lack of connectivity could cause local extinctions of certain species not mitigated by immigrant populations from neighboring patches and could interfere with pollination, seed dispersal, wildlife migration and breeding (Estreguil & Mouton, 2009).

Forest clearings change spatial patterns of forest landscapes that are readily apparent to humans, and such spatial patterns can be analyzed via their composition (the elements present) and configuration (how these elements are arranged) (Li & Reynolds, 1994; Turner, Gardner, & O'Neill, 2001). Both composition and configuration are important for a variety of ecological reasons – species survivability, species dispersal, species migration patterns – and as such, quantitative methods are required to measure these two factors, to identify their changes, and to incorporate them into research on land use land cover change.

Since 1972, large-scale deforestation analyses have become increasingly more feasible with the use of satellite imagery (Giles & Burgoyne, 2008). The rapid developments of geo-techniques, such as remote sensing and geographic information systems (GIS), have substantially advanced the collection and analysis of forest data. With assistance from remote sensing and other tools, forest studies have progressed rapidly, and in turn, forested landscapes have provided in many cases important testing grounds for the development and application of landscape ecology principles, tools and methods (Perera, Buse, & Crow, 2007), such as the theory of island biogeography and meta-population. Recently, Kupfer (2012) noted that the widely used package FRAGSTATS released two decades ago has revolutionized landscape analyses and entrenched landscape pattern indices in both the minds and toolboxes of many landscape ecologists and biogeographers. On the other hand, FRAGSTATS as well as FRAGSTATS-like metrics suffer limitations, and one major problem is the mismatch between patterns and processes (Cardille, Turner, Clayton, Gergel, & Price, 2005), where the true relationship between them is important for uncovering the controlling mechanisms of the systems. Hence, in order to better understand spatial patterns of developed areas (for simplicity, in this paper, developed areas refer to the clearance of forests or non-forest areas, whereas non-developed areas refer to forest areas) during the process of deforestation, a large collection of techniques and methodologies has been developed to solve and/or improve this shortcoming and to facilitate the understanding of deforested landscapes and their dynamics, such as moving window analysis (e.g., Riitters et al., 2002; Zurlini, Riitters, Zaccarelli, & Petrosillo, 2007), graph theory (Baggio, Salau, Janssen, Schoon, & Bodin, 2011; Bunn, Urban, & Keitt, 2000; Minor & Urban, 2008; Saura & Pascual-Hortal, 2007), normalized spectral entropy index (Sun & Southworth, 2013b; Zaccarelli, Li, Petrosillo, & Zurlini, 2012) and morphological spatial pattern analysis (MSPA) (Vogt et al., 2007). In particular, MSPA has been widely employed in landscape analyses, such as scale pattern measurement, landscape connectivity mapping, and green infrastructure detection (Ostapowicz, Vogt, Riitters, Jacek, & Christine, 2008; Sun & Southworth, 2013a; Wickham, Riitters, Wade, & Vogt, 2010).

It is logical to conclude that there is a clear trend to move from applying simple FRAGSTATS and FRAGSTATS-like landscape metrics to landscapes to the use of graphs (Kupfer, 2012), and such advancement contributes a more functional approach to landscape quantification and to the understanding of landscape dynamics. However, most often, forest fragmentation can be envisaged as a surface growth process (Barabasi & Stanley, 1995), and such complex, irregular patterns cannot be described properly by traditional Euclidean geometry but can be measured by an alternative tool – that of fractal geometry.

In this research, we will adopt a fractal analysis with a fixed-grid scans strategy (e.g., Iannaccone & Khokha, 1996) to characterize the spatial patterns of the developed areas in an Amazon landscape undergoing deforestation and development. Notably, the fixed-grid scans strategy pixelizes entire landscapes and calculates the fractal dimension within each pixel. Such pixel-level fractal cartography conforms to the current trend in landscape ecology described above. Next, a configuration scheme based on a mathematical model is proposed to partition the calculated continuous fractal dimensions into five types that are able to indicate different stages of development. The specific research questions to be addressed here are as follows: (1) What are the spatial patterns associated with the development process?; (2) Can development levels be classified from this scheme?; and (3) Does the pixel-level fractal cartography provide more insight into the patterns and processes debate than a more traditional FRAGSTATS type methodology?

Materials and methods

A deforested landscape in the Amazon: the 'MAP' region

We take up the case of the southwestern Amazon, a forested region where rapid landscape change is occurring. The center of the southwestern Amazon is a tri-national frontier: Madre de Dios, a Department of Peru, meets the state of Acre in Brazil and the department of Pando in Bolivia. Consequently, this frontier is known as the 'MAP region', and it covers an area of approximately 300,000 km^2 (Fig. 1). Though it remains 90% forested overall and contains high levels of biological and social diversity (Myers, Mittermeier, Mittermeier, da Fonseca, & Kent, 2000), the MAP region has suffered accelerated changes in its forested landscape (Southworth et al., 2011) primarily due to the construction of the Inter-Oceanic Highway (IOH), which connects central Brazil to the Pacific ports in Peru. In Acre, the paving was completed in 2002, while the paving in Madre de Dios began in 2005 and was completed in 2010. In contrast, paving of primary roads in Pando remains limited. The three states in the MAP region have differing population sizes and land use patterns, and such differences, revealed in land cover by satellite data (Perz et al., 2012, 2013),

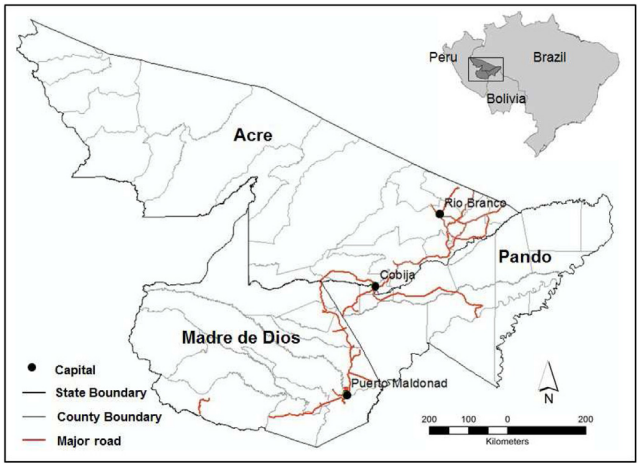

Fig. 1. Map of the study region with three capital cities and the major road superimposed. This region encompasses tri-national frontier regions of the Peruvian state of Madre de Dios, the Brazilian state of Acre, and the Department of Pando, Bolivia, termed the 'MAP' region. Note: Adapted from "Indicating structural connectivity in Amazonian rainforests from 1986 to 2010 using morphological image processing analysis," by Sun, J. & Southworth, J. (2013a), International Journal of Remote Sensing, 34, 5187–5200. Adapted with permission.

constitute a useful case to assess the performance of the proposed pixel-level fractal cartography techniques across landscapes with a range of patterns and dynamics in order to review their landscape ecology applications.

Time-series of forest cover maps can reflect the changing trajectories of forest areas and their associated fragmentation patterns (Tole, 2006). In the MAP region, six forest/non-forest maps were interpreted from Landsat 4, 5 Thematic Mapper (TM) and Landsat 7 Enhanced Thematic Mapper plus (satellite images for the years 1986, 1991, 1996, 2000, 2005, and 2010 (Paths 1–3, Rows 67–69, excluding 1/69). Acquired dates are between May and October in each year, corresponding to the dry season when cloud cover and aerosols are both low.

For consistency, we performed the same pre-processing for all images: registration, atmospheric corrections, radiometric calibration, and geometric correction to the Global Land Cover Facility Geocover product for 1999/2000. Next, these processed images were combined into a mosaic and classified into forest class and non-forest class by a decision tree classification method. Compumine Rule Discover System (RDS), a data-mining tool, was applied to create decision rules and classify the image mosaics. A tasseled cap transformation was performed to obtain three bands: brightness, greenness, and wetness, which along with a mid-infrared vegetation index and a three-by-three convolution variance image, were employed as inputs for each mosaic year. The forest class includes all dense vegetated covers, which by default, includes secondary succession as a cover type once a dense canopy is achieved. The non-forest class includes agriculture, pasture areas, cleared areas, major roads, urban fabrics, and open shrub, and these non-forest cover types are defined by the term 'developed areas'. Compumine predicts the specified land cover classes using a split-sample validation. For the MAP region, we used 85% of the training sample to create the decision tree and 15% to test the model. The rules (98.0%–99.8% accurate) were then input into the ERDAS Knowledge Engineer to produce a forest/non-forest map for all years. The classification accuracy was evaluated using over 350 training samples collected during fieldwork from 2005 to 2006, with the resulting accuracies of the Kappa coefficient, overall percent accuracy for forest and non-forest classes, and overall classification all exceeding 90% for 2005 (refer to Marsik, Stevens, & Southworth, 2011; Southworth et al., 2011 for more details). We also compared the 2000 image data with Advanced Spaceborne Thermal Emission and Reflection Radiometer (ASTER) images for the year 2000 and found an overall accuracy of 96% across our products. For 2010 data, we used Google Earth to check the results, and the overall accuracy reached 95% for the MAP region. In addition, the areas of cloud in any given year were removed from each date.

Bottom-up plan and fixed-grid scans strategy

The box-counting approach is one of the frequently used techniques to estimate fractal dimension (Mandelbrot, 1977), and a bottom-up method was adopted to calculate fractal dimension (Encarnação, Gaudiano, Santos, Tenedório, & Pacheco, 2012; Falconer, 2003) in this research. Specifically, a series of grids are repeatedly layered within an AOI box, and in each iteration '*k*', the minimum N_k squares of side $\varepsilon_k = 2^k$ (pixels, 1 pixel = 30 m) needed to encompass the developed areas were recorded, where $k = [0, \ldots, m]$ and the maximum iterations m was set as 5, which is sufficient to maintain stable results (e.g., Encarnação et al., 2012). After $m = 5$ iterations, the fractal dimension D can be estimated by a linear regression:

$$\log N_k = -D \log \varepsilon_k + c \quad (1)$$

where c is a constant. This bottom-up plan was then implemented by the fixed-grid scans strategy, which can represent fractal structures over large, heterogeneous landscapes. Essentially, a fixed-grid scans strategy pixelizes the entire landscape and then calculates the fractal dimension of each pixel. One known issue with this method is deciding what the pixel size (the length of one side of the pixel) should be because the box-counting method relies on dividing pixels recursively, and therefore, they would not often be divided exactly. In order to preserve accuracy in the calculations, as well as to maintain the finest resolution of the final graphic products as much as possible (Li, Du, & Sun, 2009), 3840 m (128 pixels) as the least common multiple of $\varepsilon_k = 2^k$, $k = [0, \ldots, 5]$ was selected as the preferred pixel (grid) size, that is, 3840 m (128 pixels) can be exactly divided by $\varepsilon_k = 2^k$, $k = [0, \ldots, 5]$ without any remainder.

Results

Remotely sensed analysis of forest cover change in the MAP region

In the MAP region, though forest cover percentage decreases from 96.1% in 1986 to 88.4% in 2010, the entire landscape is still largely forested (Fig. 2, Table 1). The percentage of developed area increases from 1.5% in 1986 to 9.2% in 2010. Clouds and water bodies were excluded for all six years and classified as one category (No Data), which accounts for approximately 2.4% of the total area. Previous research (Southworth et al., 2011) indicates very limited areas of regrowth from 1986 to 2010. Therefore, the potential inclusion of secondary succession within the forest class is almost non-existent. The dominant cover type is forest cover and the main process occurring at all three sites is that of deforestation for development (roads, homes, agriculture etc.).

Mapping fractality across the MAP region

The cartographic representations of fractal structure across the MAP region are presented in Fig. 3, and they show that the range of fractal dimensions are not evenly distributed, denoting a heterogeneous landscape. The results (Fig. 3) reveal that developed areas in the MAP region have been spreading rapidly and have become increasingly clustered over the time period from 1986 to 2010. Fig. 3 clearly shows the low fractal dimensions (more yellow) (in the web version), which represent forest or very small forest clearings, and higher fractal dimensions (more red) (in the web version), which are associated with more developed areas. The distributions of *R*-squared and standard error of the linear regression values of the calculations both support, with the large *R*-squared and small standard error values, the robust regression results and fractal structures (Appendix S1 in Supplementary material).

It is worth noting that fractal dimensions of 100% forest grids were arbitrarily set as zero and did not count in any actual calculation, and the percentage of these grids in the MAP region are 57.9%, 46.2%, 54.3%, 42.2%, 41.2% and 39.6% for the years 1986, 1991, 1996, 2000, 2005, and 2010, respectively, while the percentage of grids affected by clouds was 23.5%. In contrast, 18.6%, 30.3%, 22.2%, 34.3%, 35.3% and 36.9% of the MAP region for the years 1986, 1991, 1996, 2000, 2005, and 2010, respectively, were used in calculations relating to the developed land cover class for each of the dates.

Because deforestation changes the spatial patterns of forest cover across the landscape and species and people respond to this altered pattern in turn (Malanson, Wang, & Kupfer, 2007), it is necessary to analyze the fraction of developed areas (composition) and their associated fractal dimensions (configuration) in combination and to interpret such relationships over the time period of the deforestation process.

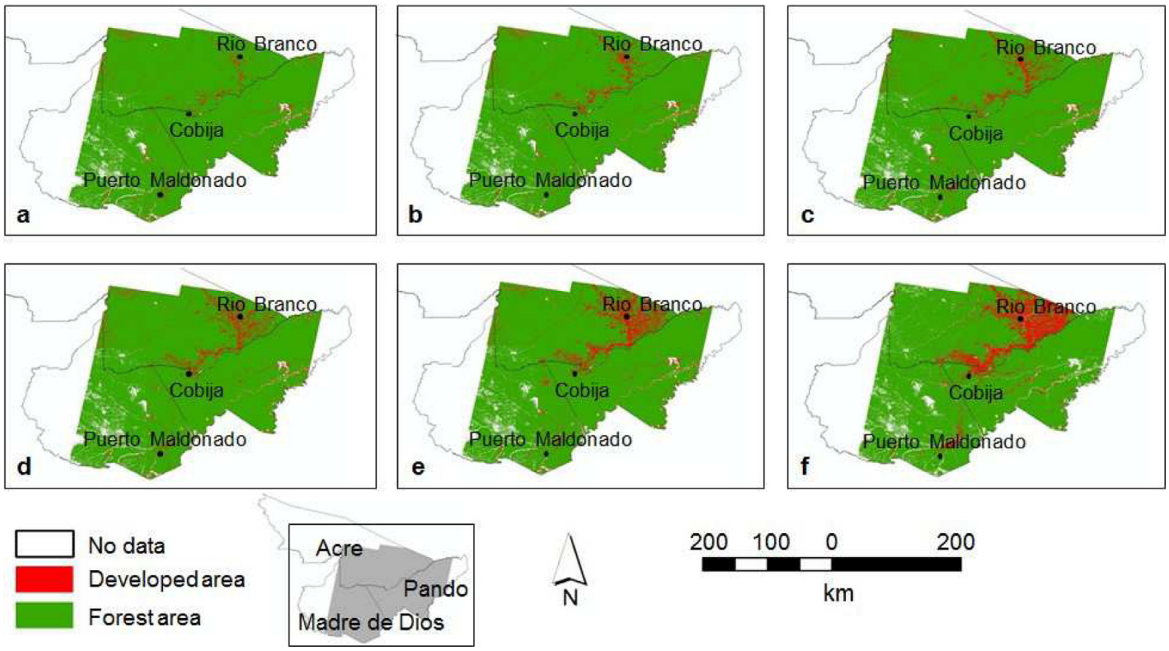

Fig. 2. Forest/non-forest maps showing clearing dynamics in the MAP region for the years a. 1986, b. 1991, c. 1996, d. 2000, e. 2005, and f. 2010, interpreted from eight Landsat images (path/row: 1/67, 1/68, 2/67, 2/68, 2/69, 3/67, 3/68, 3/69). Note: Adapted from "Indicating structural connectivity in Amazonian rainforests from 1986 to 2010 using morphological image processing analysis," by Sun, J. & Southworth, J. (2013a), International Journal of Remote Sensing, 34, 5187–5200. Adapted with permission.

Table 1
Statistical summary of forest/non-forest dynamics from 1986 to 2010.[a]

Class	1986 (%)	1991 (%)	1996 (%)	2000 (%)	2005 (%)	2010 (%)
Forest	96.1	94.6	94.4	93.3	91.2	88.4
Non-forest	1.5	3.0	3.2	4.3	6.4	9.2
No data	2.4	2.4	2.4	2.4	2.4	2.4

[a] 1% represents approximately 1655.9 km^2 in the MAP region.

Incorporating composition and configuration of developed areas in the MAP region

For the process of deforestation in the MAP region, the fraction of developed areas '*a*' in each grid was plotted as a function of the associated fractal dimension '*D*' (Fig. 4). Specifically, the total developed area '*A*' in each grid was normalized and represented by its fraction '*a*' as $a = A/A_c$, where A_c is the pixel area (e.g., 3840 m × 3840 m = 14,745,600 m^2). Zooming into the bottom-up calculation process, for iteration number k, where $k = [0, \ldots, m]$ and $m = 5$, the developed area A_k occupied by the N_k boxes with side ε_k is expressed as:

$$A_k = N_k \times \varepsilon_K^2 \tag{2}$$

thus, we can replace the N_k in Equation (1) by A_k, and developed area $A_k$is given as:

$$\log A_k = (2 - D) \times \log \varepsilon_k + c \tag{3}$$

so that we obtain $A_k = A_{k+1} \times 2^{D-2}$, which can be further inferred as:

$$A_0 = A_m \times (2^m)^{D-2} \tag{4}$$

where $k = [0, \ldots, m]$ and $m = 5$. This relationship is then used to derive the upper least bound of developed areas as a function of D:

$$U(D) = L^2 \times (2^m)^{D-2} \tag{5}$$

where L is the box length (L is 128 pixels; it is easy to infer that L^2 must be larger than or equal to any A_k, where $k = [0, \ldots, m]$ and $m = 5$). The lower least bound $L(D)$ will be proportional to the upper least bound $U(D)$, such that:

$$L(D) = \alpha \times U(D) \tag{6}$$

Considering a situation in which there is only one pixel of developed area in a grid, that is, A_k and N_k both equal to 1 in each iteration (independently of k), then the slope of the linear regression in equation (1) will be equal to zero, that is, $D = 0$. Thus, it can be concluded $L(0) = 1$ and $\alpha = (2^m/L)^2$, so that:

$$L(D) = 2^{md} \tag{7}$$

Both $U(D)$ and $L(D)$ were normalized as $u(D)$ and $l(D)$ by dividing by L^2 and then being superimposed (Fig. 6). Obviously, many cells with different fractions '*a*' correspond to the same '*D*', and vice versa. For a certain cell i on the least upper bound, that is, $a_i(D_i) = u(D_i)$, any new developed areas will inevitably increase the fractal dimension D. Conversely, when $a_i(D_i) < u(D_i)$, forest areas can still be cleared without necessarily increasing the fractal dimension. To quantitatively assess these differences across the landscape and be more informative, a configuration scheme based on a mathematical model can now be developed.

Quantitative assessment of configuration

For a given D, we computed the number of possible configurations of developed areas that meet $l(D) \le a \le u(D)$ using all the data (Fig. 4) as derived from Encarnação et al. (2012), where a function $\Omega(A, D)$ is built to compute the number of possible configurations

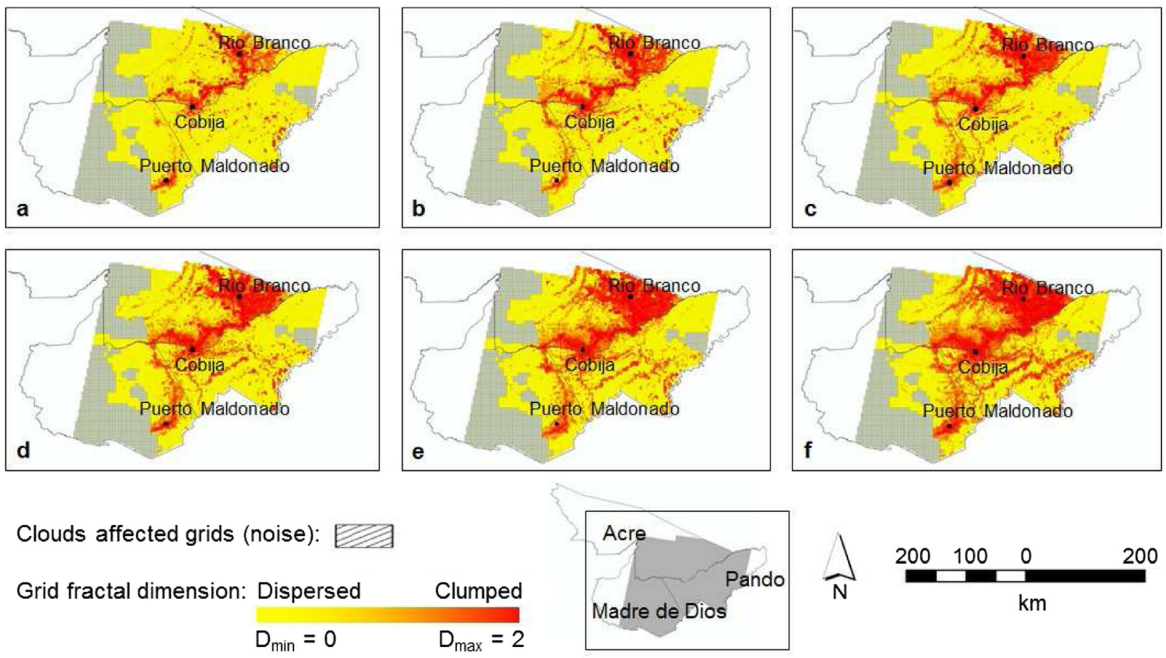

Fig. 3. Spatio-temporal fractal analysis of the developed areas in the MAP region for the years a. 1986, b. 1991, c. 1996, d. 2000, e. 2005, and f. 2010. To maintain the data quality and result accuracy, some grids were removed due to cloud influences.

within each grid characterized by developed areas '*A*' and fractal dimension '*D*'. The number of possible configurations is given by:

$$S = S(D) = \log\left(\sum_{A=L(D)}^{U(D)} \Omega(A, D)\right) \quad (8)$$

where the values of S and $S' = dS/dD$ determine different regimes that partition the data into 5 types (Fig. 5) (See Appendix S2 in Supplementary material). The quantity S can be understood as 'micro-canonical' entropy, measuring the number of possible configurations compatible with a given fractal dimension (Encarnação et al., 2012). Specifically, these types are type 1, no or trivial clearing areas; type 2, highly dispersed clearings occurring in a dominantly forested landscape; type 3, metastatic growth; type 4, rapid growth and metastatic consolidation; and type 5, clearing consolidation. Therefore, the deforestation process can be viewed as an evolutionary progression from Type 1 to Type 5.

According to this configuration scheme, different developments of developed areas across the MAP region were represented (Fig. 6) and summarized (Table 2). Among these 5 types, only Type 1 areas decreased from 62.6% in 1986 to 46.0% in 2010, and this reduction indicates that deforestation is taking place rapidly and spreading

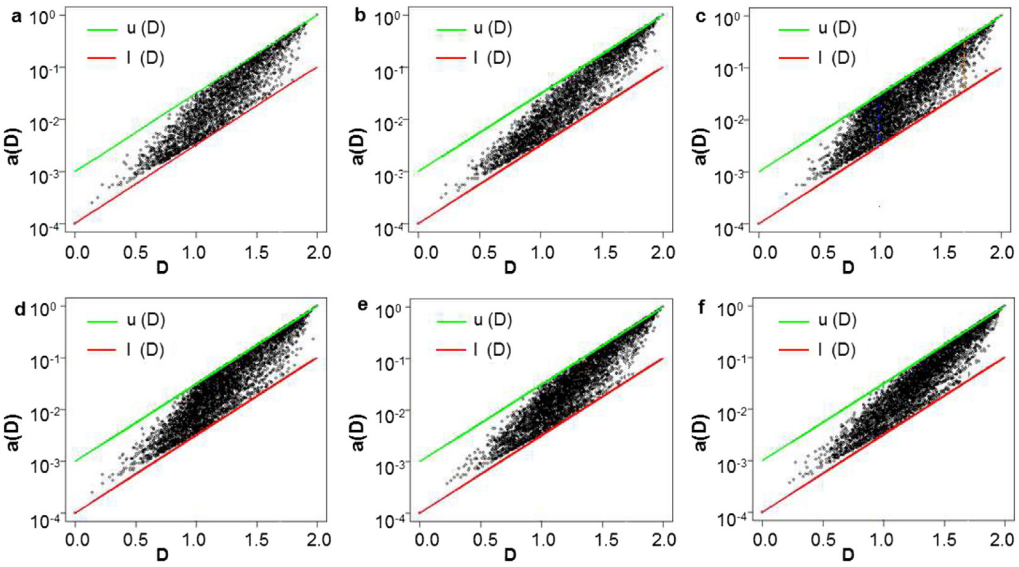

Fig. 4. Fraction of developed areas in each grid a(D) (plotted as log10 scale) as a function of the associated fractal dimension (D) for the years a. 1986, b. 1991, c. 1996, d. 2000, e. 2005, and f. 2010. All distributions are bounded by the least upper bound u(D) and lower bound l(D).

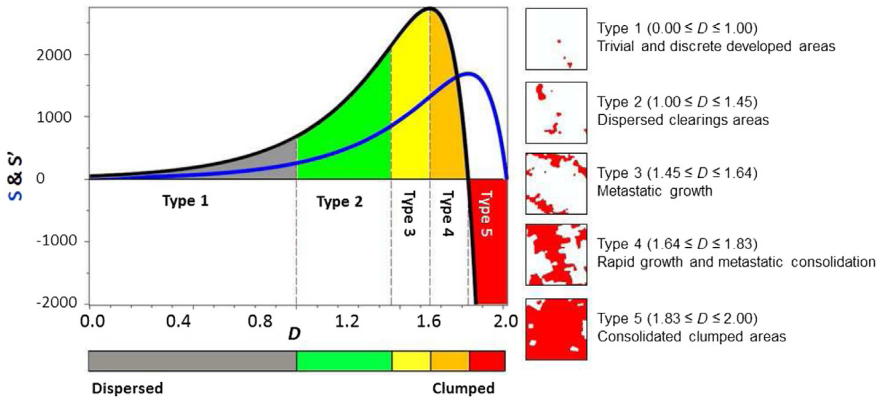

Fig. 5. Types of deforestation stages. S(D) (blue curve) and its changing rate S′(D) (black curve) were plotted with respect to the associated fractal dimension D. Five types were defined by the mathematical model and characterized in the insert maps. (For interpretation of the references to color in this figure legend, the reader is referred to the web version of this article.)

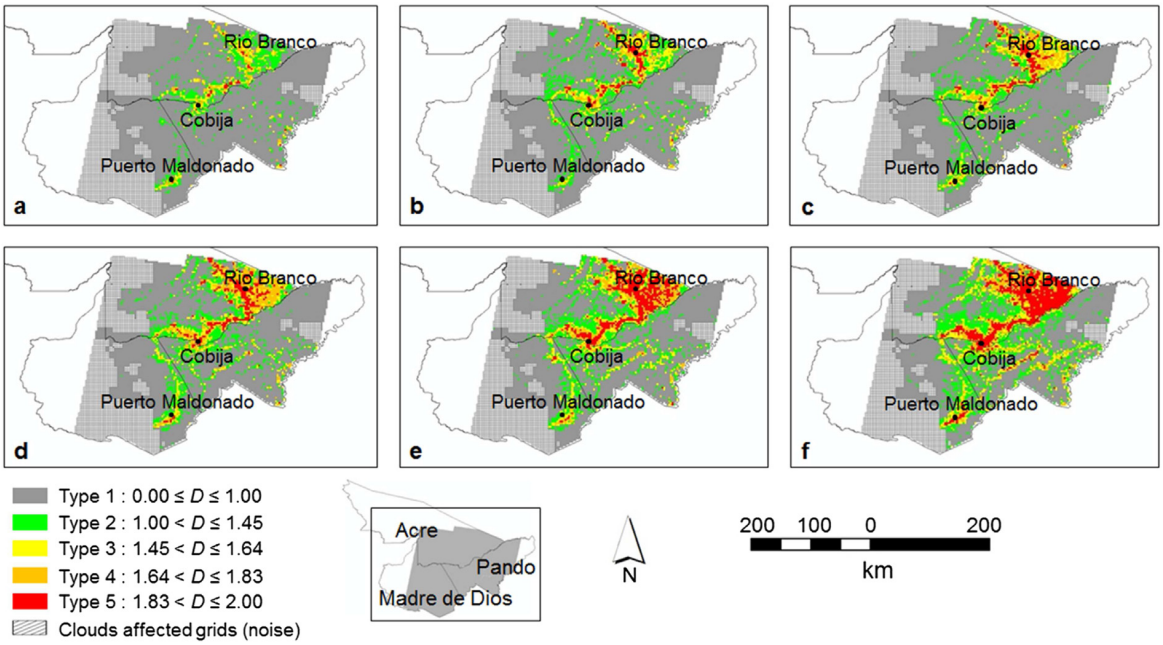

Fig. 6. The evolving pattern of development as indicated by density-sliced fractal dimension in the MAP region for the years a. 1986, b. 1991, c. 1996, d. 2000, e. 2005, and f. 2010.

extensively. Types 2–5 all experienced increases from 1986 to 2010, where Types 2, 3, and 4 have slight increases from 8.3%, 2.8%, and 2.3% in 1986 to 13.7%, 5.2%, and 5.1% in 2010. The highly developed grids, Type 5, increased from 0.4% in 1986 to 6.4% in 2010, and where such grids were initially located primarily around the three capital cities, Rio Branco (Acre), Cobija (Bolivia), and Puerto Maldonado (Peru), over time have dispersed into connected areas (Fig. 6). Such graphical representations of these stages of deforestation in the MAP region with such spatially explicit pixel-level information enable us to provide multi-level, local, adaptive, and flexible information to forest conservation groups, land managers and related programs.

Discussion

As described, the uneven distribution of forest conversions among the three states makes the heterogeneity a primary concern in the analysis, and forest landscapes deal almost exclusively with large and heterogeneous geographic areas (Perera et al., 2007). Therefore, we argue forest conservation programs should emphasize local solutions rather than a global optimization. Compared with former fractal research that only measures one or several fractal dimensions (e.g., Feng & Chen, 2010), the algorithm adopted here provides spatially explicit deforestation information at the pixel level. In addition, to make the continuous fractal dimensions more tractable numerically, a model was built to partition the fractal value range into five categories using a mathematical function (Encarnação et al., 2012). The deforestation process can then be viewed as an evolutionary development, and with such clear definition, policy makers and conservationists can regulate different management strategies to address different problems or predict some potential effects. The five types and their dynamics illustrated in the final resultant map reflect different development levels among the three states in the study area, both spatially and

Table 2
Statistical summary of region type dynamics from 1986 to 2010.[a]

Class	1986 (%)	1991 (%)	1996 (%)	2000 (%)	2005 (%)	2010 (%)
Type 1	62.6	55.2	60.5	50.6	48.9	46.0
Type 2	8.3	13.0	7.8	15.3	14.5	13.7
Type 3	2.8	3.8	3.1	3.7	4.3	5.2
Type 4	2.3	3.2	3.8	4.7	4.6	5.1
Type 5	0.4	1.3	1.4	2.2	4.3	6.4
Cloud affected grids	23.5	23.5	23.5	23.5	23.5	23.5

[a] 1% represents approximately 1655.9 km^2.

temporally. Considering these five stages, ranging from no or minimal development to highly developed, we argue types 2, 3, and 4 should be highlighted in conservation planning, as they represent transitional areas where the shrunken interior forest and the expanded cleared area meet. Therefore, conservation programs or even restoration activities should focus on these unsteady intermediate regions, as they provide a window of opportunity to understand deforestation processes, dynamics and effects at a clearly defined level.

The fractal methodology carried out in this paper can be used to understand deforestation and urbanization, which provides an alternative perspective to the spatial methods devised to date. We think the methodology described has great potential to provide new insights to current conservation and/or urban planning programs. By creating large fractal pictures of study landscapes, we can identify environmental hot-spots, cold-spots, and intermediate regions in order to provide different recommendations to policymakers.

On the other hand, though easy to measure, fractal analysis can cause misunderstandings, such as the differences between monofractal and multi-fractal, self-similar and self-affine. Particularly, the appreciation of the multi-fractal should be emphasized and clarified in future research, which may be able to reveal useful information, such as urban growth. Fractal analysis, as a newly emerging branch of mathematics, must be undertaken under strict mathematical derivation and must be cautiously used when applied to real world problems.

Again, the Amazonian rainforest is undergoing significant land cover changes, transitioning from forest to urban and agriculture lands (DeFries, Foley, & Asner, 2004; Laurance et al., 2001). Targeting regional integrations (to improve accessibility), many forms of infrastructure — particularly transportation — have been heavily subsidized, such as the IOH, which was introduced to link Atlantic ports in Brazil and Pacific ports in Peru (Perz et al., 2013). For example, soybean production in Brazil, which plays a key role in the country's economic development, has increased dramatically, and Brazil may overtake the USA as the world's top soybean producer (Arvor, Dubreuil, Simões, & Bégué, 2013; Liu et al., 2013). In order to compete with USA soybean exports, more roads may be planned in the future to reduce road transportation cost, as well as to access remote resources in Brazil. Increased road construction, in turn, may cause substantial impacts on the environment, such as increased intensity of agricultural land use and forest loss. Though not 'palatable', road construction could lead people to a better life. Without government legislation and intensive conservation efforts, we would argue that many Amazon forest areas may continue to be encroached upon until they reach the level of fractal dimension 2.

Acknowledgments

Special thanks are due to Yanguang Chen and Jiejing Wang, both of whom introduced Jing Sun to the arena of fractal geometry. This research was funded as part of an NSF Human and Social Dynamics Program (FY2005) project titled "Agents of Change: Infrastructure Change, Human Agency, and Resilience in Social-Ecological Systems" #0527511 and also by NSF Coupled Natural Human Systems # 1114924, "Global sensitivity and uncertainty analysis in the evaluation of social-ecological resilience: Theoretical debates over infrastructure impacts on livelihoods and forest change".

Appendix A. Supplementary data

Supplementary data related to this article can be found at http://dx.doi.org/10.1016/j.apgeog.2014.05.011.

References

Arvor, D., Dubreuil, V., Simões, M., & Bégué, A. (2013). Mapping and spatial analysis of the soybean agricultural frontier in Mato Grosso, Brazil, using remote sensing data. *GeoJournal, 78*, 833–850.
Baggio, J., Salau, K., Janssen, M., Schoon, M., & Bodin, O. (2011). Landscape connectivity and predator prey population dynamics. *Landscape Ecology, 26*, 33–45.
Barabasi, A. L., & Stanley, H. E. (1995). *Fractal concepts in surface growth* (1st ed.). Cambridge: Cambridge University Press.
Bunn, G., Urban, L., & Keitt, H. (2000). Landscape connectivity: a conservation application of graph theory. *Journal of Environmental Management, 59*, 265–278.
Cardille, J., Turner, M., Clayton, M., Gergel, S., & Price, S. (2005). METALAND: characterizing spatial patterns and statistical context of landscape metrics. *Bioscience, 55*, 983–988.
DeFries, R. S., Foley, J. A., & Asner, G. P. (2004). Land-use choices: balancing human needs and ecosystem function. *Frontiers in Ecology and the Environment, 2*(5), 249–257.
Encarnação, S., Gaudiano, M., Santos, C., Tenedório, J., & Pacheco, J. (2012). Fractal cartography of urban areas. *Scientific Reports, 2*, 527.
Estreguil, C., & Mouton, C. (2009). *Measuring and reporting on forest landscape pattern, fragmentation and connectivity in Europe: Methods and indicators*. JRC Scientific and Technical report EUR23841EN. Office for Official Publications of the European Communities.
Falconer, K. J. (2003). *Fractal geometry: Mathematical foundations and applications*. New York: John Wiley & Sons Inc.
Fearnside, P. M. (2004). Greenhouse gas emissions from hydroelectric dams: controversies provide a springboard for rethinking a supposedly "clean" energy source. *Climatic Change, 66*, 1–8.
Feng, J., & Chen, Y. G. (2010). Spatiotemporal evolution of urban form and land use structure in Hangzhou, China: evidence from fractals. *Environment and Planning B: Planning and Design, 37*, 838–856.
Giles, P. T., & Burgoyne, J. M. (2008). Skole, D.L. and Tucker, C.J. 1993: tropical deforestation and habitat fragmentation in the Amazon: satellite data from 1978 to 1988. Science 260, 1905—1910. *Progress in Physical Geography, 32*, 575–580.
Gunderson, L., & Holling, C. S. (2002). *Panarchy: Understanding transformations in human and natural systems* (1st ed.). Washintong, D.C: Island Press.
Gutman, G., Janetos, A., Justice, C., Moran, E., Mustard, J., Rindfuss, R., et al. (2004). *Land change science: Observing, monitoring, and understanding trajectories of change on the earth's surface*. New York: Kluwer Academic Publishers.
Hanski, I., & Ovaskainen, O. (2003). Metapopulation theory for fragmented landscapes. *Theoretical Population Biology, 64*, 119–127.
Iannaccone, P. M., & Khokha, M. (1996). *Fractal geometry in biological systems: An analytical approach* (1st ed.). New York: CRC-Press.
Kupfer, J. A. (2012). Landscape ecology and biogeography. *Progress in Physical Geography, 36*, 400–420.
Lambin, E. F., & Geist, H. J. (2006). *Land-use and land cover change: Local processes and global impacts*. New York: Springer.
Laurance, W. F., Albernaz, A., Schroth, G., Fearnside, P. M., Bergen, S., Venticinque, E. M., et al. (2002). Predictors of deforestation in the Brazilian Amazon. *Journal of Biogeography, 29*, 737–748.
Laurance, W. F., Cochrane, M. A., Bergen, S., Fearnside, P. M., Delamônica, P., Barber, C., et al. (2001). The future of the Brazilian Amazon. *Science, 291*(5503), 438–439.
Li, J., Du, Q., & Sun, C. (2009). An improved box-counting method for image fractal dimension estimation. *Pattern Recognition, 42*, 2460–2469.
Lima, A., Silva, T. S., Aragão, L. E., Feitas, R. M., Adami, M., Formaggio, A. R., et al. (2012). Land use and land cover changes determine the spatial relationship between fire and deforestation in the Brazilian amazon. *Applied Geography, 34*, 239–246.
Li, H., & Reynolds, J. F. (1994). A simulation experiment to quantify spatial heterogeneity in categorical maps. *Ecology, 75*, 2446–2455.
Liu, J., Hull, V., Batistella, M., DeFries, R., Dietz, T., Fu, F., et al. (2013). Framing sustainability in a telecoupled world. *Ecology and Society, 18*(2), 26.
Malanson, G. P., Wang, Q., & Kupfer, J. A. (2007). Ecological processes and spatial patterns before, during and after simulated deforestation. *Ecological Modelling, 202*, 397–409.

Malhi, Y., Roberts, J. T., Betts, R. A., Killeen, T. J., Li, W., & Nobre, C. A. (2008). Climate change, deforestation, and the fate of the Amazon. *Science, 319*, 169–172.
Mandelbrot, B. B. (1977). *Fractals, form, chance and dimension*. San Francisco: W.H. Freeman and Company.
Marsik, M., Stevens, F., & Southworth, J. (2011). Amazon deforestation: rates and patterns of land cover change and fragmentation in Pando, northern Bolivia, 1986 to 2005. *Progress in Physical Geography, 35*, 353–374.
Messina, J. P., Walsh, S. J., Mena, C. F., & Delamater, P. L. (2006). Land tenure and deforestation patterns in the Ecuadorian amazon: conflicts in land conservation in frontier settings. *Applied Geography, 26*(2), 113–128.
Minor, E. S., & Urban, D. L. (2008). A graph-theory framework for evaluating landscape connectivity and conservation planning. *Conservation Biology, 22*, 297–307.
Myers, N., Mittermeier, R. A., Mittermeier, C. G., da Fonseca, G. A. B., & Kent, J. (2000). Biodiversity hotpots for conservation priorities. *Nature, 403*, 853–858.
Nepstad, D., Carvalho, G., Barros, C. A., Alencar, A., Capobianco, J. P., Bishop, J., et al. (2001). Road paving, fire regime feedbacks, and the future of Amazon forests. *Forest Ecology and Management, 154*, 395–407.
Nobre, P., Malagutti, M., Urbano, D. F., de Almeida, R. A. F., & Giarolla, E. (2009). Amazon deforestation and climate change in a coupled model simulation. *Journal of Climate, 22*, 5686–5697.
Ostapowicz, K., Vogt, P., Riitters, K., Jacek, K., & Christine, E. (2008). Impact of scale on morphological spatial pattern of forest. *Landscape Ecology, 23*, 1107–1117.
Perera, A., Buse, L., & Crow, T. (2007). *Forest landscape Ecology: Transferring knowledge to practice* (1st ed.). New York: Springer.
Perz, S. G., Cabrera, L., Carvalho, L. A., Castillo, J., Chacacanta, R., Cossio, R., et al. (2012). Regional integration and local change: road paving, community connectivity and social-ecological resilience in a tri-national frontier, Southwestern Amazonia. *Regional Environmental Change, 12*, 35–53.
Perz, S. G., Qiu, Y., Xia, Y., Southworth, J., Sun, J., Marsik, M., et al. (2013). Transboundary infrastructure and land cover change: highway paving and community-level deforestation in a tri-national frontier in the amazon. *Land Use Policy, 34*, 27–41.
Riitters, K. H., Wickham, J. D., O'Neill, R. V., Jones, K. B., Smith, E. R., Coulston, J. W., et al. (2002). Fragmentation of continental United States forests. *Ecosystems, 5*, 0815–0822.
Saura, S., & Pascual-Hortal, L. (2007). A new habitat availability index to integrate connectivity in landscape conservation planning: comparison with existing indices and application to a case study. *Landscape and Urban Planning, 83*, 91–103.
Scheffer, M., Bascompte, J., Brock, W. A., Brovkin, V., Carpenter, S. R., Dakos, V., et al. (2009). Early-warning signals for critical transitions. *Nature, 461*, 53–59.
Scheffer, M., Carpenter, S., Foley, J. A., Folke, C., & Walker, B. (2001). Catastrophic shifts in ecosystems. *Nature, 413*, 591–596.
Southworth, J., Marsik, M., Qiu, Y., Perz, S., Cumming, G. S., Stevens, F., et al. (2011). Roads as drivers of change: trajectories across the Tri-National frontier in MAP, the southwestern Amazon. *Remote Sensing, 3*, 1047–1066.
Sun, J., & Southworth, J. (2013a). Indicating structural connectivity in Amazonian rainforests from 1986 to 2010 using morphological image processing analysis. *International Journal of Remote Sensing, 34*, 5187–5200.
Sun, J., & Southworth, J. (2013b). Retrospective analysis of landscape dynamics using normalized spectral entropy. *Remote Sensing Letters, 4*(11), 1049–1056.
Tole, L. (2006). Measurement and management of human-induced patterns of forest fragmentation: a case study. *Environmental Management, 37*, 788–801.
Turner, M. G., Gardner, R. H., & O'Neill, R. V. (2001). *Landscape ecology in theory and practice: Pattern and process*. New York: Springer.
Vogt, P., Riitters, K., Estreguil, C., Kozak, J., Wade, T., & Wickham, J. (2007). Mapping spatial patterns with morphological image processing. *Landscape Ecology, 22*, 171–177.
Wickham, J., Riitters, K., Wade, T., & Vogt, P. (2010). A national assessment of green infrastructure and change for the conterminous United States using morphological image processing. *Landscape and Urban Planning, 94*, 186–195.
Zaccarelli, N., Li, B.-L., Petrosillo, I., & Zurlini, G. (2012). Order and disorder in ecological time-series: introducing normalized spectral entropy. *Ecological Indicators, 28*, 22–30.
Zurlini, G., Riitters, K., Zaccarelli, N., & Petrosillo, I. (2007). Patterns of disturbance at multiple scales in real and simulated landscapes. *Landscape Ecology, 22*, 705–721.